Gonzalez, E. A., Dorčák, U., Monje, C. A., Valsa, J., Caluyo, F. S. & Petráš, I. (2014). Conceptual design of a selectable fractional-order differentiator for industrial applications. Fractional Calculus and Applied Analysis, 17(3), 697-716.

DOI: 10.2478/s13540-014-0195-z

**SURVEY PAPER**

# CONCEPTUAL DESIGN OF A SELECTABLE FRACTIONAL-ORDER DIFFERENTIATOR FOR INDUSTRIAL APPLICATIONS

**Emmanuel A. Gonzalez [1], Ľubomír Dorčák [2], Concepción A. Monje [3], Juraj Valsa [4], Felicito S. Caluyo [5], Ivo Petráš [2]**



**Abstract**

In the past decade, researchers working on fractional-order systems modeling and control have been considering working on the design and development of analog and digital fractional-order differentiators, i.e. circuits that can perform non-integer-order differentiation. It has been one of the major research areas under such field due to proven advantages over its integer-order counterparts. In particular, traditional integer-order proportional-integral-derivative (PID) controllers seem to be outperformed by fractional-order PID (FOPID or $PI^{\lambda}D^{\mu}$) controllers. Many researches have emerged presenting the possibility of designing analog and digital fractional-order differentiators, but only restricted to a fixed order. In this paper, we present the conceptual design of a variable fractional-order differentiator in which the order can be selected from 0 to 1 with an increment of 0.05. The analog conceptual design utilizes operational amplifiers and resistor-capacitor ladders as main components, while a generic microcontroller is introduced for switching purposes. Simulation results through Matlab and LTSpiceIV show that the designed resistor-capacitor ladders can perform as analog fractional-order differentiation.

*MSC 2010*: Primary 26A33; Secondary 65D25, 65D30, 93C05, 93C55

*Key Words and Phrases*: fractional calculus, fractional-order differentiator, fractional-order controller, Matlab

## 1. Introduction

The use of industrial controllers such as proportional-integral-derivative (PID) controllers are ubiquitous in the chemical, electrical and mechanical industries. Such controllers have been constructed and designed to help plant maintenance technicians and engineers maintain the desired performances of their systems by incorporating these modules in feedback and forward loops. These commercially available PID controllers are tunable at a certain extent and evidences from current suppliers and manufacturers of these devices show that such controllers are becoming better and better with additional communication and signal handling capabilities. One of the areas for improvement of such controllers is having the ability to incorporate fractional-order dynamics which could only be introduced using a fractional-order PID (FOPID) controller. Conceptually, FOPID controllers are composed of three modules: 1) a proportional (amplifier) module; 2) a fractional-order differentiator (FOD) module; and 3) a fractional-order integrator (FOI) module, all of which are connected in parallel. This paper focuses on the FOD module.

FODs are differentiators that perform non-integer-order differentiation, e.g. $\frac{1}{2}$-order differentiation which gets the half-derivative of a function. The term *fractional-order*, though construed to have order values between 0 and 1, is actually a misnomer because it pertains to differentiation having an arbitrary order that is not necessarily between 0 and 1. Furthermore, the order could also be negative in value making the system an FOI.

The study of fractional-order differentiators and integrators have been existing since the late 1600's (see e.g. in [18]) and it has gained research momentum in the 80's and 90's due to mathematical discoveries showing that fractional-order differentiators and integrators are ubiquitous in various science and engineering fields, such as those in the biomedical, controls and automation, signals and systems, electrical and mechanical system industries, [17, 19, 26]. In fact, the number of researches in fractional-order differentiators and integrators and its application in various fields have drastically increased since the year 2000 and there is already a widespread of applications for such field—which is evidently shown in the increased number of conferences and publications in this area, [3, 5, 6, 4, 13, 23, 26]. Fractional-order differentiators and integrators are products of fractional calculus—the theory of differentiation and integration in arbitrary order.

Performing fractional-order differentiation on function $f(t)$ can be done using the Riemann-Liouville (RL) definition as

$$ {}_{RL}D^{\alpha} f(t) \triangleq \frac{d^m}{dt^m} \left\{ \frac{1}{\Gamma(m-\alpha)} \int_0^t \frac{f(\tau)}{(t-\tau)^{\alpha-m+1}} d(\tau) \right\}, \tag{1.1} $$

where $m-1 < \alpha < m$, $m \in \mathbb{N}$, $\alpha$ is the fractional-order of differentiation, and $\Gamma(\cdot)$ is the usual Euler's gamma function. An alternative representation called the Grunwald-Letnikov (GL) definition is in the form of

$$ \begin{aligned} {}_{GL}D^{\alpha} f(t) &\triangleq \sum_{k=0}^{m} \frac{f^{(k)}(0^+)\, t^{k-\alpha}}{\Gamma(m+1-\alpha)} + \frac{1}{\Gamma(m+1-\alpha)} \\ &\times \int_0^t (t-\tau)^{m-\alpha} f^{(m-1)}(\tau)\, d\tau, \end{aligned} \tag{1.2} $$

where, $m > \alpha - 1$, see e.g. [25].

The Laplace transform of the RL definition is

$$ \mathcal{L}\{{}_{RL}D^{\alpha} f(t)\} = s^{\alpha} F(s) - \sum_{k=0}^{m-1} s^k \left[ {}_{RL}D^{\alpha-k-1} f(t) \right]_{t=0}, \tag{1.3} $$

while the Laplace transform of the GL definition is

$$ \mathcal{L}\{{}_{GL}D^{\alpha} f(t)\} = s^{\alpha} F(s). \tag{1.4} $$

In the case in which the initial conditions are zero, the Laplace transforms of both definitions result in the common form of

$$ \mathcal{L}\{D^{\alpha} f(t)\} = s^{\alpha} F(s). \tag{1.5} $$

In this paper, we present the conceptual designs of the analog electronic realization of an FOD of order $0 < \alpha < 1$ having an equivalent continuous-time transfer function of

$$ F(s) = s^{\alpha}, \tag{1.6} $$

in which the order $\alpha$ is selectable between 0 and 1 with an increment of 0.05 units. We show that the design of such FODs can be done using analog operational amplifiers (op-amps) and a resistor-capacitor ladder network for the analog circuitry.

The organization of this paper is as follows. Section **2** presents the theory behind the continuous-time implementations of fractional-order differentiators. In Section **3**, the conceptual analog implementation of an FOD is presented, while simulations results are presented in Section **4**. Practical aspects that need to be considered for industrial use are presented in Section **5**. Finally, Section **6** presents some conclusions and recommendations for further study in this area.

## 2. Theory and Realization of Fractional-Order Elements

Fractional-order elements such as FODs have a constant magnitude slope of $20\alpha$ dB per decade, and a flat horizontal phase at $\alpha\pi/2$ radians, where $\alpha > 0$ is the order of differentiation, [22, 29]. This result can be derived by directly getting the magnitude and phase spectrum of (1.6). FOD is also ideally known as a constant phase element (CPE)—a model that is seen to be ubiquitous in the field of biomedical engineering especially on sensor-tissue impedance studies, [9, 16, 24].

An FOD can be electronically realized by having an infinite number of lumped-sum RC networks [22] representing an ideal transmission line which is practically impossible to achieve due to the infinite number of components. It was reported that such FOD can be represented using continued fraction expansions (CFE) [27] expressed by rational functions of the Laplace independent variable $s$ – resulting in an infinite RC ladder network (see Fig. 1), [7, 11]. However, by limiting the frequency range of application for the CPE, one can design a module composed of a finite number of components such as a finite ladder by truncating the CFE [22] that can approximately work as a CPE for the specific range of interest, and eventually become a practically–acceptable FOD [20, 21] for various applications.

The Oustaloup filter is one of the most widely-used and common analog filter representations for a fractional-order element. An Oustaloup filter is expressed as [20]:

$$F(s) = K \prod_{k=1}^{N} \frac{s + \omega_k^{'}}{s + \omega_k}, \tag{2.1}$$

in which the parameters are evaluated through the zeros $\omega_k^{'} = \omega_b \omega_u^{(2k-1-\alpha)}$, the poles $\omega_k = \omega_b \omega_u^{(2k-1+\alpha)}$, and the gain $K = \omega_h^{\alpha}$. The parameter $\omega_u = \sqrt{\omega_h/\omega_b}$ is the average of the low and high cut-off frequencies $\omega_b$ and $\omega_h$, respectively, and $\alpha$ is the order of the desired differentiator. Furthermore, it can be seen in (2.1) that the number of poles and zeros are equal, and would depend on the order $N$ of the filter. The value of the filter order $N$ can be either even or odd.

The idea of the Oustaloup filter is to generate a combination of lead and lag components, ideally spaced in the entire frequency spectrum, in order to approximate a magnitude response with a slope of $20\alpha$ dB/dec. In order to get a good approximation of an FOD using the Oustaloup filter, it is important to consider the number of poles and zeros which is dictated by the filter order $N$.

The Oustaloup filter can be simulated using Matlab with the following script [17]:

```
function G=ousta_fod(gam,N,wb,wh)
k=1:N; wu=sqrt(wh/wb);
wkp=wb*wu.^((2*k-1-gam)/N);
wk=wb*wu.^((2*k-1+gam)/N);
G=zpk(-wkp,-wk,wh^gam); G=tf(G);
```

which determines an $N$-th order filter to approximate a fractional-order differentiator of order $\gamma$, having the low and high cut-off frequencies $\omega_b$ and $\omega_h$, respectively. A modified version of the Oustaloup filter has been proposed [31] to improve its FOD approximation characteristics in higher frequency bandwidths, but is not anymore discussed in this paper.

The use of RC ladders [8, 30] have been exercised since the mid-20th century for realizing fractional-order elements [1, 7, 10, 11], but the approximation results were disappointing—having only a very limited bandwidth with a high number of components. An improved version of the RC ladder was introduced in [28] and has shown to be superior over its predecessors having only a small amount of components needed to perform as a CPE at a better bandwidth. The concept in [28] have been applied recently for the realization of fractional-order systems, [5, 6].

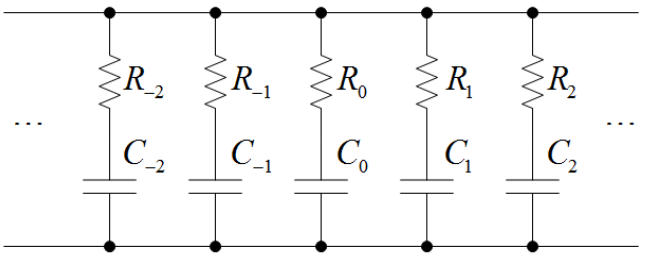


FIGURE 1. A typical infinite RC ladder.

A typical RC ladder is shown in Fig. 1 which is composed of a parallel combination of series RC networks. If these resistor-capacitor values are designed in such a way that they form the power sequences

$$R_k = R_0 a^k \tag{2.2}$$

and

$$C_k = C_0 b^k, \tag{2.3}$$

in which $0 < a < 1$, $0 < b < 1$, and $-\infty < k < \infty$ for integer values of $k$, then they will form a logarithmic scale of poles and zeros that will approximate an Oustaloup filter. In [28], the RC ladder was modified because the

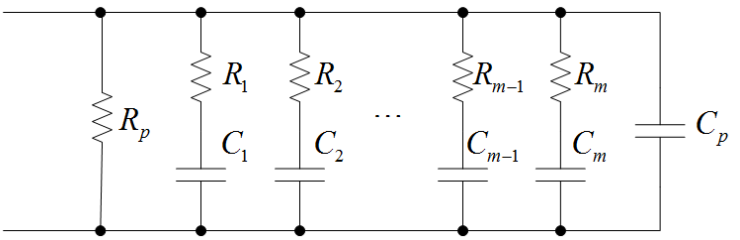


FIGURE 2. The improved RC ladder with $R_p$ (2.5), $C_p$ (2.6), and branch resistor-capacitor network values from (2.7) and (2.8).



previous representation required too many components to realize, in this case, an FOI of the form

$$F(s) = s^{-\alpha} \tag{2.4}$$

for a certain frequency of interest, and decreasing its complexity was found to be necessary. In particular, it was found that the left-hand side of the RC ladder dictates the low cut-off frequency $\omega_{min} > 0$ and is more resistive in nature, while the right-hand side dictates the high cut-off frequency $\omega_{max} > \omega_{min}$ having a dominant capacitive effect. The left-hand side can then be represented by a single resistor

$$R_p = R_1 \frac{1-a}{a}, \tag{2.5}$$

while the right-hand side can be similarly represented by a capacitor

$$C_p = C_1 \frac{b^m}{1-b}, \tag{2.6}$$

where $m > 0$ is the number of RC ladder branches to be designed. The branch resistance and capacitance values become

$$R_k = R_1 a^k \tag{2.7}$$

and

$$C_k = C_1 b^k, \tag{2.8}$$

respectively for $k = 0, 1, 2, \cdots, m$. The resulting improved RC ladder in [28] is shown in Fig. 2.

The relationship between the resistors and capacitors with low and high cut-off frequencies are dictated by

$$\omega_{min} \approx \frac{1}{R_1 C_1} \tag{2.9}$$

and

$$\omega_{max} \approx \frac{\omega_{min}}{(ab)^m}, \tag{2.10}$$

respectively. Since the ladder will only approximate an FOI at frequencies $\omega_{min}$ to $\omega_{max}$, a certain ripple will exist. The ripple in the form of variations in the phase can be associated with the variables $a$ and $b$ as

$$ab \approx \frac{0.24}{1+\Delta\varphi}, \tag{2.11}$$

where $\triangle\varphi$ is the phase ripple in degrees. The relationship of the variables $a$ and $b$ with the order of integration $\alpha$ is defined by

$$\log a = \alpha \log (ab), \tag{2.12}$$

as a direct result from [2]. The resulting admittance of the improved RC ladder becomes

$$Y(j\omega) = \frac{1}{R_p} + j\omega C_p + \sum_{k=1}^{m} \frac{j\omega C_k}{1 + j\omega R_k C_k}. \tag{2.13}$$

The slope of the magnitude of impedance by inverting (2.13) is proportional to the order $\alpha$ of the integrator and its magnitude value at $\omega = 1$ is determined using

$$D = \frac{1}{|Y(j\omega_{av})|\, \omega_{av}^{\alpha}}, \tag{2.14}$$

where

$$\omega_{av} = \sqrt{\omega_{min}\omega_{max}} \tag{2.15}$$

is the average frequency. In the case where it is necessary to have an FOI of the form

$$F(s) = D_r s^{-\alpha}, \tag{2.16}$$

it is necessary to recalibrate all resistance values by multiplying it by $D_r/D$, and similarly dividing all capacitors with the same ratio. It is by necessary for $D_r$ to be an acceptably large value, especially when incorporating it in operational amplifier circuits, as discussed in the next section.

## 3. Conceptual Design of the FOD

The motivation on designing a selectable fractional-order differentiator comes from the idea of creating an industry-grade fractional order PID controller where the gain of the proportional controller, and gains and orders of the differentiator and integrator controllers are selectable. In this particular research, the discussion is focused on the FOD module and that its gain is set to be at unity gain, i.e. 0 dB.

The overall architecture of the conceptual FOD is shown in Fig. 3. The entire system has an analog input and an analog output. The maximum

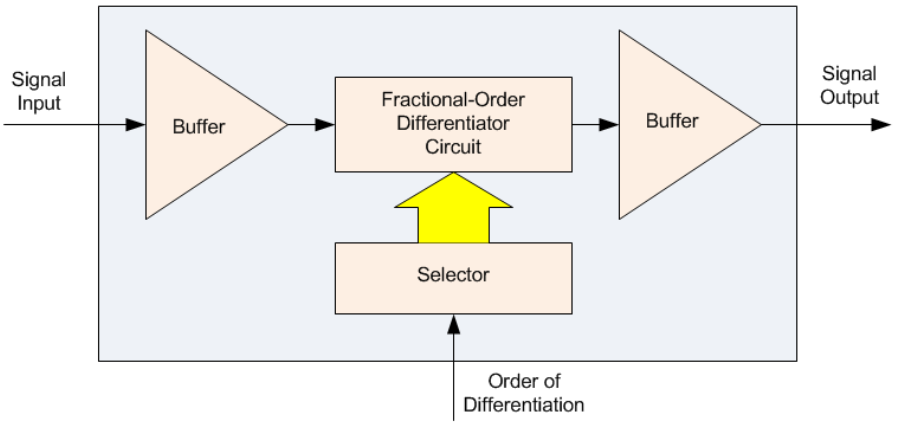


FIGURE 3. Conceptual design (architecture) of a selectable fractional-order differentiator.

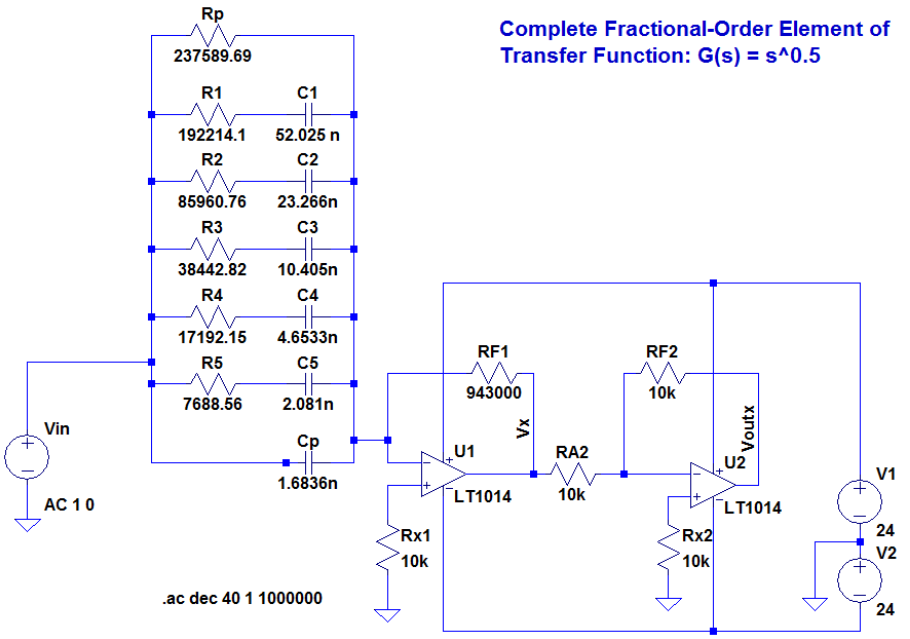


FIGURE 4. Analog circuit design of a fractional-order differentiator of order $\alpha = 0.5$.

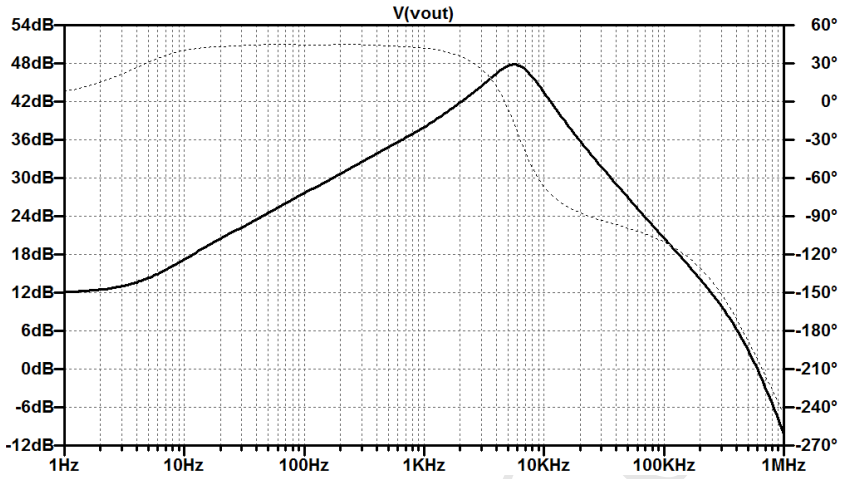


FIGURE 5. Magnitude (solid line) and phase (dashed line) spectra of a fractional-order differentiator of order $\alpha = 0.5$.

output swing of the input and output voltages shall be determined by the characteristics of the input and output buffer circuits. If the input signal to the system is $x(t) = A\sin(\omega t)$, then the output signal becomes $y(t) = B\sin(\omega t - \varphi)$, where the ratio $B/A = \omega^{\alpha}$ and the phase difference in radians $\varphi = \alpha\pi/2$ are determined by the order of differentiation $0 < \alpha < 1$, where $\omega > 0$ is the radian frequency of the input signal. The order of integration is also selectable input from 0 to 1 with a step increment of 0.05. Therefore, there are 21 possible orders to choose from.

### 3.1. RC Ladder Design

The conceptual design of the RC ladder starts with the identification of the maximum allowable phase ripple $\Delta\varphi$ in degrees, desired gain of the differentiator $D_r$, order of the differentiator $\alpha$, number of RC ladder branches $m$, and initial values of $R_1$ and $C_1$. A complete RC ladder design will only serve for one fractional order. Therefore, separate ladder circuits are needed for every selected order $\alpha$. Since there are 19 possible orders of differentiation, which excludes 0 (buffer) and 1 (differentiator), there should be 19 separate RC ladder circuits to be designed.

For a semi-differentiator ($\alpha = 0.5$) example, consider the following assumptions: $\Delta\varphi = 0.2°$, $D_r = 10^3$, $m = 5$, $R_1 = 10^4\ \Omega$ and $C_1 = 1\ \mu$F. From (2.11), the product $ab$ can be obtained as

$$ab = \frac{0.24}{1 + \Delta\varphi} = \frac{0.24}{1 + 0.2} = 0.2. \tag{3.1}$$

The range of frequency of operation can now be obtained through (2.9) as

$$\omega_{min} \approx \frac{1}{R_1 C_1} = \frac{1}{(10^4)\,(10^{-6})} = 100\,\text{rad/s}, \tag{3.2}$$

and through (2.10) as

$$\omega_{max} \approx \frac{\omega_{min}}{(ab)^m} = \frac{100}{(0.2)^5} = 312500\,\text{rad/s}. \tag{3.3}$$

The individual parameters $a$ and $b$ can be obtained from (2.12) as

$$a = 10^{\alpha \log(ab)} = 10^{(0.5)\log(0.2)} = 0.44721, \tag{3.4}$$

and

$$b = \frac{ab}{a} = \frac{0.2}{0.44721} = 0.44721. \tag{3.5}$$

From these results, the primary resistor and capacitor values can then be calculated from (2.5) and (2.6) as

$$R_p = R_1 \frac{1-a}{a} = \left(10^5\right) \frac{1 - 0.44721}{0.44721} = 12360.68\,\Omega, \tag{3.6}$$

and

$$C_p = C_1 \frac{b^m}{1-b} = \left(10^{-6}\right) \frac{(0.44721)^5}{1 - 0.44721} = 32.361\,\text{nF}, \tag{3.7}$$

respectively. Using (2.7) and (2.8), the rest of the branch resistance and capacitance values are then computed as follows: $R_2 = 4.47\,\text{k}\Omega$, $R_3 = 2.0\,\text{k}\Omega$, $R_4 = 894\,\Omega$, $R_5 = 400\,\Omega$, $C_2 = 447\,\text{nF}$, $C_3 = 200\,\text{nF}$, $C_4 = 89.4\,\text{nF}$, and $C_5 = 40\,\text{nF}$. Using (2.15), the average frequency can be calculated as

$$\omega_{av} = \sqrt{\omega_{min}\omega_{max}} = \sqrt{(100)\,(312500)} = 5590.2\,\text{rad/s}. \tag{3.8}$$

The average impedance can be obtained by inverting (2.13) and using the Matlab script:

```
Rp=12360.6789; Cp=3.2361e-8;
wav=5590.2;
C=[1e-6 4.47e-7 2e-7 8.94e-8 4e-8];
R=[1e4 4.47e3 2e3 8.94e2 4e2];
Yp=1/Rp+i*wav*Cp; Y=0;
for k = 1,length(C)
Y=Y+(i*wav*C(k))/(1+i*wav*C(k)*R(k));
end
Ytot=Y+Yp; Zav=1/abs(Ytot)
```

and the resulting average impedance is obtained as $Z_{av} = 3889.8\,\Omega$. Using this result, the magnitude value from (2.14) becomes

$$D = \frac{1}{|Y(j\omega_{av})|\,\omega_{av}^{\alpha}} = \frac{1}{(3889.8)\,(5590.2)^{0.5}} = 66.0568\,\Omega. \tag{3.9}$$

The ratio $D_r/D$ to calibrate the resistance and capacitance values in the ladder results in

$$\frac{D_r}{D} = \frac{10^3}{66.0568} = 15.13848. \tag{3.10}$$

Multiply the ratio (3.10) in the resistor values and divide the same ratio to the capacitor values, and it will result in: $R_p = 237589.6889\,\Omega$, $R_1 = 192214.10\,\Omega$, $R_2 = 85960.76\,\Omega$, $R_3 = 38442.82\,\Omega$, $R_4 = 17192.15\,\Omega$, $R_5 = 7688.56\,\Omega$, $C_p = 1.6836\,\text{nF}$, $C_1 = 52.025\,\text{nF}$ $C_2 = 23.266\,\text{nF}$, $C_3 = 10.405\,\text{nF}$, $C_4 = 4.6533\,\text{nF}$, and $C_5 = 2.081\,\text{nF}$.

In order for the ladder to function as part of an FOD, it should be incorporated in the arm of an inverting operational amplifier (op-amp) circuit since the circuit's ideal transfer function is

$$G(s) = -\frac{Z_F(s)}{Z_A(s)}, \tag{3.11}$$

where $Z_F(s)$ is the feedback impedance and $Z_A(s)$ is the arm impedance which will be represented by the ladder circuit having the transfer function (2.4). Incorporating (2.4) into (3.11) will result in

$$G(s) = -\frac{Z_F(s)}{s^{-\alpha}} = -Z_F(s)\, s^{\alpha}. \tag{3.12}$$

In the assumption that the feedback impedance is purely resistive, i.e. $Z_F(s) = R_F$, and that the system in (3.12) is post-cascaded to another inverting amplifier, it can be seen that the overall circuit becomes a complete FOD of the form

$$G(s) = R_F s^{\alpha}. \tag{3.13}$$

The circuit of the designed FOD is shown in Fig. 4. The value of $R_F$ in (3.13), which is $R_{F1}$ in Fig. 4, must be chosen such that the entire FOD's magnitude is naturalized as 0 dB at $\omega = 1$ rad/s. However, since the ladder circuit may not perform very well at $\omega = 1$ rad/s given that its minimum assumed frequency of operation is $\omega_{min} \approx 100$ rad/s, it is more practical to calibrate the FOD circuit at the average frequency in (3.8), which is around 890 Hz. Since the nearest decade point is at 1 kHz, the magnitude gain of the FOD should be at $|G(j\omega)|_{\omega=2\pi(1000)} = \omega^{0.5}\big|_{\omega=2\pi(1000)} = 79.2665$ which is around 37.98 dB. With this calibration point, the feedback resistor $R_F$ is identified to work at $R_F \approx 945\,\text{k}\Omega$. The frequency response of the FOD is shown in Fig. 5.

From Fig. 5, the range of operation in which the FOD is applicable is between 10 Hz to around 1 kHz, instead of 16 Hz ($\omega_{min} = 100$ rad/s) to 50 kHz ($\omega_{max} = 312500$ rad/s). This is due to the characteristics and limitations of the op-amps used which are two LT1014 quad precision op-amps [15]. According to [15], the gain-bandwidth-product (GBP)

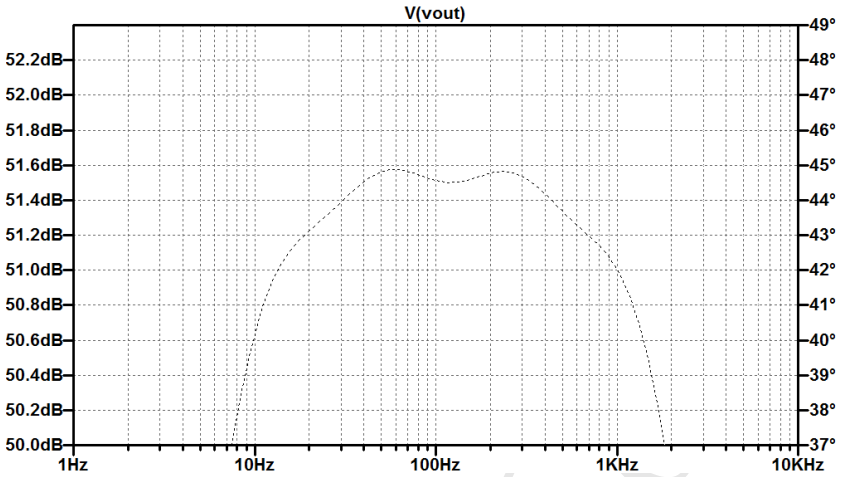


FIGURE 6. Zoomed phase spectrum of a fractional-order differentiator of order $\alpha = 0.5$ focusing on the phase angle.

of an LT1014 op-amp is 1 MHz. This means that the operational amplifier at 10 kHz will only work properly with a gain of 100 (40 dB). However, the theoretical magnitude gain of an FOD circuit with $\alpha = 0.5$ is $|G(j\omega)|_{\omega=2\pi(10000)} = \omega^{0.5}\big|_{\omega=2\pi(10000)} = 250.66$ (47.98 dB), which is beyond the capability of the op-amp chosen. For higher bandwidth applications, an op-amp with a higher GBP can be selected.

It can also be seen in Fig. 5 that the phase angle between 10 Hz to around 1 kHz is approximately 45 degrees. This is revealed in Fig. 6.

### 3.2. Selector Module

The selector module block diagram is shown in Fig. 7. The module is composed of a microcontroller that acquires the designed order $\alpha$ from the user. The acquired order is then processed to provide the address of the multiplexer-demultiplexer tandem that should be selected. The address shall require $\lceil \log 21 / \log 2 \rceil = 5$ bits to operate. Due to the fact that the selected gain would require the change of ladder and feedback resistor circuits, there will be two sets of multiplexer-demultiplexer tandems for both the arm and feedback paths of the op-amp (see Fig. 8).

In Fig. 7, each FOE block is composed of a set of components corresponding to the order $\alpha$ that is being selected. For example, the block named "FOE (0.5)" denotes the circuit needed to perform differentiation of fractional order $\alpha = 0.5$. In this particular case, the "FOE (0.5)" block will contain the RC ladder in Fig. 4 for the arm path. For the feedback path, on the other hand, the "FOE (0.5)" block will contain the 743 kΩ resistor.

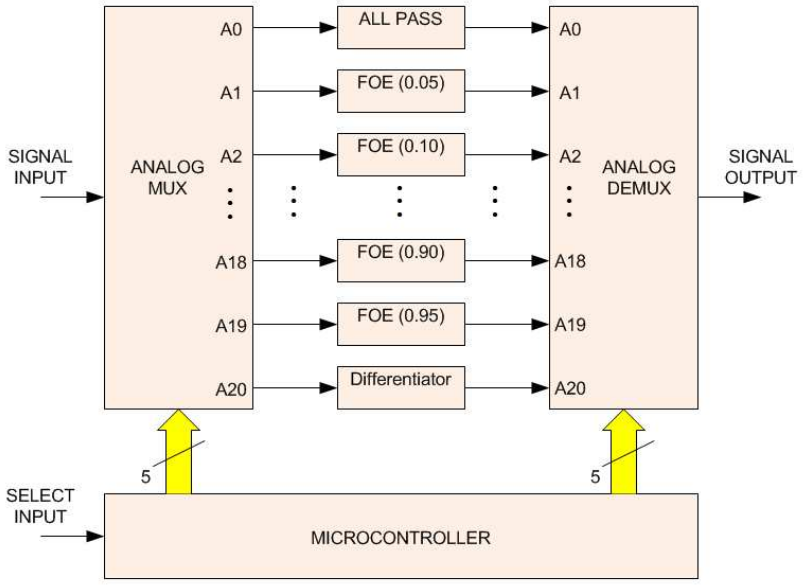


FIGURE 7. Conceptual block diagram of the selector circuit for the arm and feedback paths of the op-amp circuit.

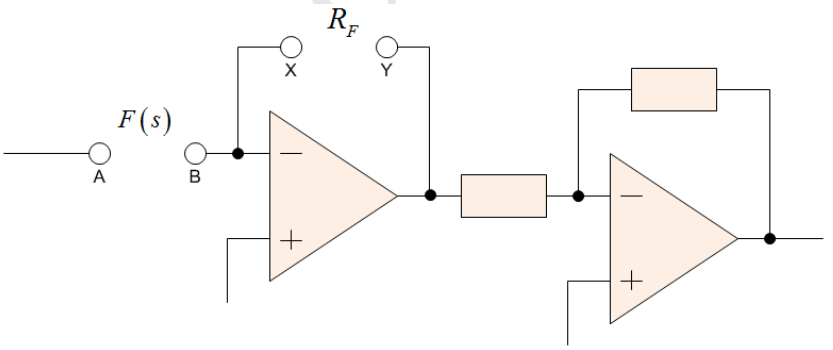


FIGURE 8. Generic schematic diagram of the op-amp circuit in which the arm and feedback paths are connected to the selector circuit through pins A and B for the arm, and pins $X$ and $Y$ for the feedback path.

### 3.3. Buffer Modules

The analog buffers are just simple op-amp-based practical buffers having high input impedance and low output impedance. In this conceptual

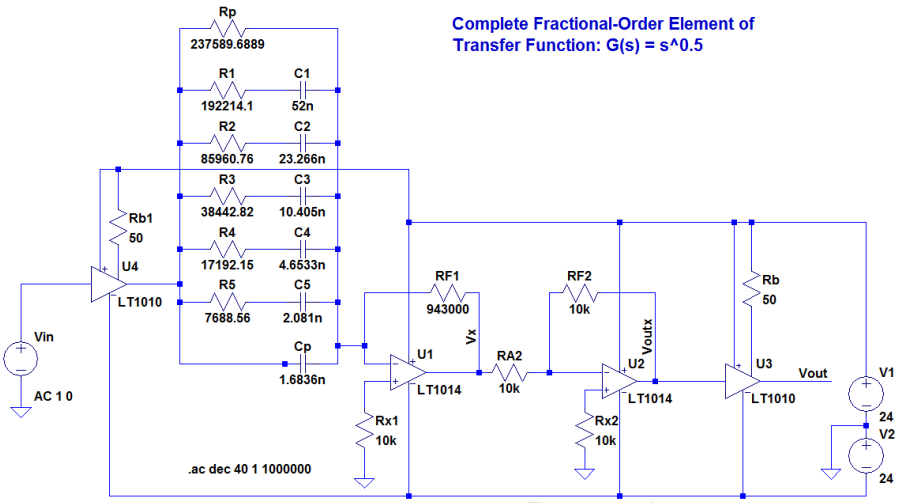


FIGURE 9. Analog circuit design of a fractional-order differentiator of order $\alpha = 0.5$ with input and output buffers using LT1014.

design, the LT1010 fast ±150 mA power buffer [14] is selected. The purpose of these buffers is just to make sure that the FOD circuit will not be affected by the input signal and the output load. The complete circuit of a half-differentiatior including the buffers is shown in Fig. 9.

## 4. Simulation Results

Tables 1 and 2 lists all resistor and capacitor values for various orders $\{0.05, 0.10, \cdots, 0.90, 0.95\}$ of differentiation. Like in the case of the $\alpha = 0.5$ example in Section **3**, each FOD was calibrated at the average frequency resulting in various values of feedback resistor $R_F$, which are shown in Table 3 for some selected orders of differentiation. The frequency responses of the FOD for fractional orders $\alpha = 0.25$ and $\alpha = 0.75$ are shown in Figs. 10 and 11, simulating the transfer functions $G_{0.25}(s) = \sqrt[4]{s}$ and $G_{0.75}(s) = \sqrt[4]{s^3}$, respectively. It can be seen from Fig. 10 that the magnitude's slope in the applicable frequencies are running at 5 dB/dec, while a slope of 15 dB/dec is seen in Fig. 11. Finally, the phase plots reveal that the FODs are able to ensure 22.5 and 67.5 degrees for FOD orders $\alpha = 0.25$ and $\alpha = 0.75$, respectively.

## 5. Other Practical Considerations

Practical considerations play a role when it comes to higher orders of differentiation. It can be seen from Table III that the feedback resistor

| $\alpha$ | $R_p$ | $R_1$ | $R_2$ | $R_3$ | $R_4$ | $R_5$ |
|---|---|---|---|---|---|---|
| 0.05 | 1668.45 | 19910.26 | 18370.81 | 16950.40 | 15639.81 | 14430.55 |
| 0.10 | 2783.81 | 15942.20 | 13572.24 | 11554.59 | 9836.88 | 8374.53 |
| 0.15 | 4645.47 | 17013.27 | 13364.18 | 10497.76 | 8246.15 | 6477.47 |
| 0.20 | 7754.68 | 20421.57 | 14801.14 | 10727.56 | 7775.12 | 5635.25 |
| 0.25 | 12959.34 | 26162.04 | 17495.61 | 11700.02 | 7824.28 | 5232.41 |
| 0.30 | 21725.78 | 35004.51 | 21598.97 | 13327.30 | 8223.39 | 5074.11 |
| 0.35 | 36747.65 | 48578.12 | 27656.75 | 15745.69 | 8964.42 | 5103.67 |
| 0.40 | 63644.66 | 70430.35 | 36997.46 | 19434.97 | 10209.30 | 5363.00 |
| 0.45 | 370080.22 | 259988.78 | 107280.58 | 44267.77 | 18266.45 | 7537.38 |
| 0.50 | 237589.69 | 192214.10 | 85960.76 | 38442.82 | 17192.15 | 7688.56 |
| 0.55 | 553744.48 | 389016.61 | 160522.03 | 66237.07 | 27331.76 | 11278.05 |
| 0.60 | 1440066.68 | 885362.48 | 337084.75 | 128338.54 | 48862.43 | 18603.43 |
| 0.65 | 399602.36 | 216395.86 | 76018.35 | 26704.72 | 9381.18 | 3295.54 |
| 0.70 | 1152133.60 | 552537.19 | 179094.61 | 58050.17 | 18815.88 | 6098.82 |
| 0.75 | 342949.14 | 146327.99 | 43762.28 | 13087.97 | 3914.22 | 1170.62 |
| 0.80 | 1061952.69 | 404723.26 | 111681.74 | 30818.12 | 8504.14 | 2346.68 |
| 0.85 | 349782.30 | 119478.51 | 30420.43 | 7745.35 | 1972.04 | 502.10 |
| 0.90 | 1292016.85 | 396725.83 | 93200.33 | 21894.98 | 5143.65 | 1208.37 |
| 0.95 | 6344335.89 | 1755778.09 | 380581.89 | 82494.81 | 17881.55 | 3876.0 |

TABLE 1. List of all resistor values in ohms for various differentiator orders $\alpha = \{0.05, 0.10, 0.15, \cdots, 0.85, 0.90, 0.95\}$.

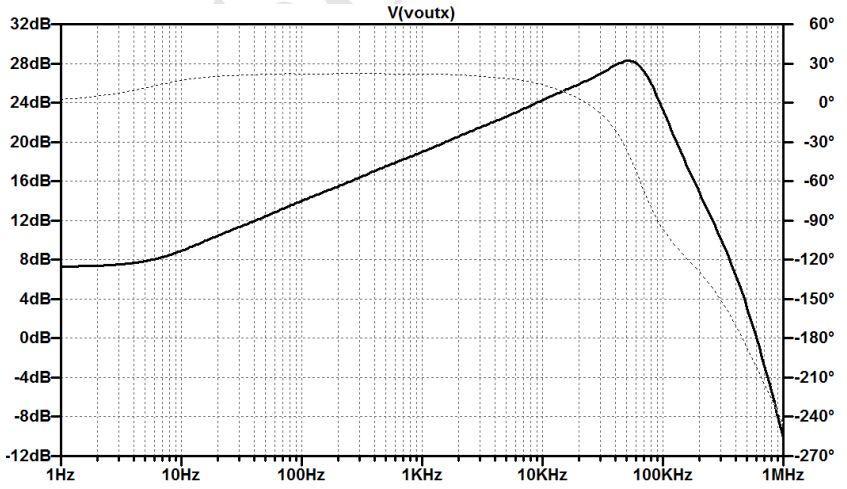


FIGURE 10. Magnitude (solid line) and phase (dashed line) spectra of a fractional-order differentiator of order $\alpha = 0.25$.

value $R_F$ increases exponentially by the order $\alpha$. For an order of $\alpha = 0.95$, the feedback resistor becomes too large because enough compensation is

| $\alpha$ | $C_p$ | $C_1$ | $C_2$ | $C_3$ | $C_4$ | $C_5$ |
|---|---|---|---|---|---|---|
| 0.05 | 0.30685 | 502.25 | 108.87 | 23.598 | 5.1152 | 1.1088 |
| 0.10 | 0.58665 | 627.27 | 147.36 | 34.618 | 8.1327 | 1.9106 |
| 0.15 | 0.84374 | 587.78 | 149.65 | 38.103 | 9.7015 | 3.4701 |
| 0.20 | 1.0821 | 489.68 | 135.12 | 37.287 | 10.289 | 2.8393 |
| 0.25 | 1.3047 | 382.23 | 114.31 | 34.188 | 10.225 | 3.0579 |
| 0.30 | 1.5122 | 285.68 | 92.597 | 30.014 | 9.7283 | 3.1533 |
| 0.35 | 1.6977 | 205.85 | 72.315 | 25.404 | 8.9242 | 3.1350 |
| 0.40 | 1.8342 | 141.98 | 54.058 | 20.581 | 7.8360 | 2.9834 |
| 0.45 | 1.9966 | 38.463 | 18.643 | 9.0359 | 4.3796 | 2.1228 |
| 0.50 | 1.6836 | 52.025 | 23.266 | 10.405 | 4.6533 | 2.0810 |
| 0.55 | 1.3344 | 25.706 | 12.459 | 6.0389 | 2.9270 | 1.4187 |
| 0.60 | 0.95175 | 12.295 | 5.9332 | 3.1168 | 1.6372 | 0.86006 |
| 0.65 | 6.4181 | 46.212 | 26.309 | 14.979 | 8.5277 | 4.8550 |
| 0.70 | 4.2269 | 18.098 | 11.167 | 6.8906 | 4.2517 | 2.6235 |
| 0.75 | 27.593 | 68.340 | 45.701 | 30.562 | 30.438 | 13.668 |
| 0.80 | 17.955 | 24.708 | 17.908 | 12.979 | 9.4072 | 6.8181 |
| 0.85 | 116.70 | 83.697 | 65.745 | 51.644 | 40.567 | 31.866 |
| 0.90 | 75.828 | 24.206 | 21.459 | 18.269 | 15.553 | 13.241 |
| 0.95 | 49.261 | 5.6955 | 5.2551 | 4.8488 | 4.4739 | 4.1280 |

TABLE 2. List of all capacitor values in $nF$ for various differentiator orders $\alpha = \{0.05, 0.10, 0.15, \cdots, 0.85, 0.90, 0.95\}$.

| $\alpha$ | $R_F$ | $\alpha$ | $R_F$ |
|---|---|---|---|
| 0.05 | 2020 | 0.90 | 3.80 M |
| 0.50 | 943 k | 0.95 | 12.00 M |

TABLE 3. List of all feedback resistor values in ohms for various differentiator orders $\alpha = \{0.05, 0.5, 0.90, 0.95\}$.



needed to ensure that the theoretical gain of the FOD at $\omega = 1$ rad/s is 0 dB. Aside from this fact, the bandwidth of operation of the designed FOD for higher orders tends to decrease because of the GBP limitations [15] of the chosen op-amp. This makes the bandwidth decrease by one decade, having the FOD operate only until 100 Hz. However, for lower orders like $\alpha = 0.05$, the high frequency could reach up to 100 kHz.

In Section **3**, it was emphasized that the tuning of the FOD can be done through $R_F$ by looking into the $\omega_{av}$ in (2.15). However, when it comes to higher orders of differentiation, the use of (2.15) may not be valid anymore due to the GBP limitations of the op-amp used. In this case, instead of using (2.15) outright, it would be necessary to get first the magnitude response of the circuit and graphically select a frequency point of reference

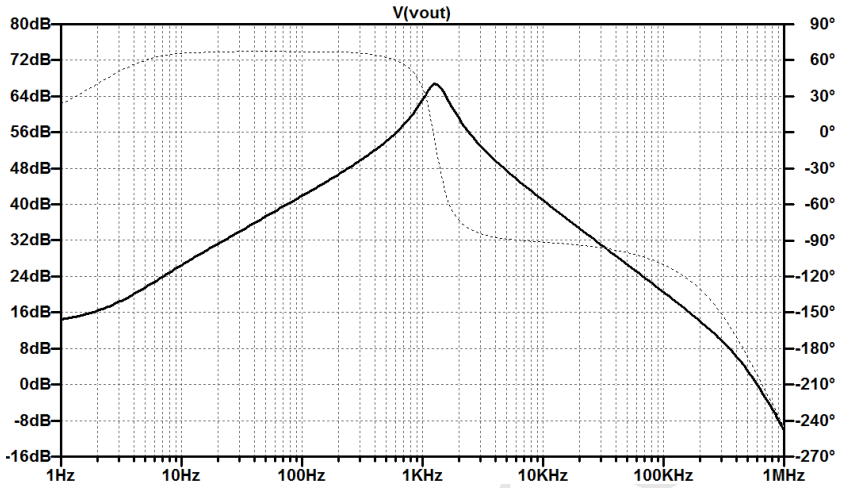


FIGURE 11. Magnitude (solid line) and phase (dashed line) spectra of a fractional-order differentiator of order $\alpha = 0.75$.

within the applicable range. In the case of this research, since the normal operation of an FOD is only until up to around 300 Hz, it may be necessary to choose a lower frequency point of reference such as 50 Hz or 100 Hz when calibrating $R_F$.

## 6. Conclusions

In this paper, we have shown that it is possible to design a fractional-order differentiator in which the order can be selected between 0 to 1 with an increment of 0.05. Theoretically, the RC ladder can perform the desired constant phase element through the order $\alpha$; however when incorporated in an op-amp circuit, the range of frequencies diminishes due to the gain-bandwidth product limitations of the op-amp used. In order to compensate for the correct gain of the differentiator at $\omega = 1$ rad/s, it is necessary to find a frequency point in which the differentiator will work well, and then adjust the feedback resistor $R_F$ accordingly. Finally, it is recommended to use an op-amp having a GBP of at least 100 MHz and find the appropriate resistor-capacitor combinations to obtain practical values that are commercially available.

The authors would also like to propose exploring the design and implementation of such fractional-order differentiators in the analog microelectronics scale.

**Acknowledgments**

This work was in part supported by grants VEGA 1/0552/14, 1/0729/12, 1/2578/12, 1/0497/11, and APVV-0482-11 from the Slovak Grant Agency, and the Slovak Research and Development Agency, respectively.

**References**

[1] G.E. Carlson, C.A. Halijak, Approximation of fractional capacitors $(1/s)^{1/n}$ by regular Newton process. *IEEE Trans. Circuit Theory* **11**, No 2 (1964), 210–213.

[2] A. Charef, H.H. Sun, Y.Y. Tsao, B. Onaral, Fractal system as represented by singularity function. *IEEE Trans. Automat. Control* **37**, No 9 (1992), 1465–1470.

[3] Y.Q. Chen, I. Petráš, D. Xue, Fractional order control - a tutorial. In: *Proc. Amer. Control Conference*, St. Louis, Missouri (2009), 1397–1411.

[4] L. Dorčák, E.A. Gonzalez, J. Terpák, I. Petráš, M. Žecová, Application of PID retuning methods for laboratory feedback control systems incorporation fractional-order dynamics. In: *14th Int. Carpathian Control Conference (ICCC 2013)*, Rytro, Poland, May 26-29 (2013), 38–42.

[5] L. Dorčák, J. Terpák, I. Petráš, J. Valsa, E. Gonzalez, Comparison of the electronic realization of the fractional-order system and its model. In: *13th Int. Carpathian Control Conference (ICCC 2012)*, High Tatras, Podbanske, Grand Hotel Permon, Slovak Republic, May 28-31 (2012), 119–124.

[6] L. Dorčák, J. Terpák, I. Petráš, J. Valsa, P. Horovčák, E. Gonzalez, Electronic realization of fractional-order system. In: *Proc. Int. Multidisciplinary Scientific GeoConference (SGEM 2012)*, Albena Resort, Bulgaria, Jun. 17-23 (2012).

[7] S.C. Dutta Roy, On the realization of a constant-argument immitance of fractional operator. *IEEE Trans. Circuit Theory* **14**, No 3 (1967), 264–374.

[8] R.K.H. Galvo, S. Hadjiloucas, K.H. Kienitz, H.M. Paiva, R.J.M. Afonso, Fractional order modeling of large three-dimensional RC networks. *IEEE Trans. Circuits and Syst. I, Regular Papers* **60**, No 3 (2013), 624–637.

[9] E.A. Gonzalez, L. Dorčák, C.B. Co, Bioelectrochemodels with fractional calculus. *Int. J. Intelligent Control and Syst.* **17**, No 1 (2012), 7–13.

[10] B.T. Krishna, Studies on fractional order differentiators and integrator: A survey. *Signal Processing* **91**, No 9 (2011), 386–426.

[11] B.T. Krishna, K. V. V. S. Reddy, Active and passive realization of fractance device of order 1/2. *Active and Passive Electronic Components* **2008** (2008), Article ID 369421, 5 pp.; DOI: 10.1155/2008/369421.

[12] B.T. Krishna, K. V. V. S. Reddy, Design of fractional order digital differentiators and integrators using indirect discretization, *Fract. Calc. Appl. Anal.* **11**, No 2 (2008), 143–151; http://www.math.bas.bg/∼fcaa.
[13] P. Lanusse, J. Sabatier, PLC implementation of a CRONE controller. *Fract. Calc. Appl. Anal.* **14**, No 4 (2011), 505–523;
DOI: 10.2478/s13540-011-0031-7;
http://link.springer.com/article/10.2478/s13540-011-0031-7.
[14] *Linear Technology.* LT1010 Fast ±150mA Power Buffer Datasheet, LT 0511 Rev. E, 1010fe.
[15] *Linear Technology.* LT1013/LT1014 Quad Precision Op Amp (LT1014) Dual Precision Op Amp (LT1013) Datasheet, LT 0510 Rev. D, 10134fd.
[16] R. Magin, *Fractional Calculus in Bioengineering.* Begell House, Inc., Connecticut (2006).
[17] C.A. Monje, Y.Q. Chen, B.M. Vinagre, D. Xue, V. Feliu, *Fractional-Order Systems and Controls: Fundamentals and Applications.* Springer, London (2010).
[18] K.B. Oldham, J. Spanier, *The Fractional Calculus.* Dover Publications, Inc., New York (2002).
[19] A. Oustaloup, P. Lanusse, J. Sabatier, P. Melchior, CRONE control: Principles, extensions and applications. *Journal of Applied Nonlinear Dynamics* **2**, No 3 (2013), 207–223.
[20] A. Oustaloup, F. Levron, B. Mathieu, F.M. Nanot, Frequency band complex non integer differentiator: characterization and synthesis. *IEEE Trans. Circuits and Syst. I, Fundam. Theory Appl.* **47**, No 1 (2000), 25–40.
[21] A. Oustaloup, B. Mathieu, *La Commande CRONE: du Scalaire au Multivariable.* Hermes, Paris (1995).
[22] I. Petráš, I. Podlubny, P. O'Leary, L. Dorčák, B.M. Vinagre, *Analogue Realizations of Fractional Order Controllers.* Faculty BERG, Technical University of Košice, Košice (2002).
[23] I. Petráš, Tuning and implementation methods for fractional-order controllers. *Fract. Calc. Appl. Anal.* **15**, No 2 (2012), 282–303;
DOI: 10.2478/s13540-012-0021-4;
http://link.springer.com/article/10.2478/s13540-012-0021-4.
[24] R. Plonsey, *Bioelectric Phenomena.* McGraw-Hill, New York (1969).
[25] I. Podlubny, *Fractional Differential Equations.* Academic Press, San Diego (1999).
[26] J. Sabatier, O.P. Agrawal, J.A. Tenreiro Machado, *Advanced in Fractional Calculus: Theoretical Developments and Applications in Physics and Engineering.* Springer, Netherlands (2007).

[27] S. Skale, S. Doleček, M. Slemnik, Substitution of the constant phase element by Warburg impedance for protective coatings. *Corrosion Sci.* **49**, No 3 (2007), 1045–1055.

[28] J. Valsa, P. Dvořák, M. Friedl, Network model of the CPE. *Radioengineering* **20**, No 3 (2011), 619–626.

[29] B. Vinagre, I. Podlubny, A. Hernandez, V. Feliu, Some approximations of fractional order operators used in control theory and applications. *Fract. Calc. Appl. Anal.* **3**, No 3 (2000), 231–248.

[30] J.C. Wang, Realizations of generalized Warburg impedance with RC ladder networks and transmission lines. *J. Electrochem. Soc.* **34**, No 8 (1987), 1915–1920.

[31] D. Xue, C.N. Zhao, Y.Q. Chen, A modified approximation method of fractional order systems. In: *Proc. IEEE Conf. on Mechatronics and Automation*, Luoyang, China (2006), 1043–1048.

[1] *Existing Installation Department, Jardine Schindler Elevator Corporation*
*8/F Pacific Star Bldg., Sen. Gil Puyat Ave. cor. Makati Ave.*
*Makati City, 1209 PHILIPPINES*
*e-mail: emm.gonzalez@delasalle.ph*

[2] *Institute of Control and Informatization of Production Processes*
*Faculty of BERG, Technical University of Košice*
*B. Němcovej 3, 042 00 Košice, SLOVAKIA*
*e-mails: lubomir.dorcak@tuke.sk ,*
*ivo.petras@tuke.sk*
*Received: February 25, 2014*

[3] *Systems Engineering and Automation Department*
*University Carlos III de Madrid, 28911 Leganés Madrid, SPAIN*
*e-mail: cmonje@ing.uc3m.es*

[4] *Brno University of Technology*
*Antonínská 1, 602 00 Brno, CZECH Republic*
*e-mail: valsa@feec.vutbr.cz*

[5] *School of Electrical, Electronics and Computer Engineering*
*Mapua Institute of Technology, Muralla St.*
*Intramuros Manila, 1000 PHILIPPINES*
*e-mail: fscaluyo@mapua.edu.ph*

---

Please cite to this paper as published in:

*Fract. Calc. Appl. Anal.*, Vol. **17**, No 3 (2014), pp. 697–716;
DOI: 10.2478/s13540-014-0195-z